Estuarine, Coastal and Shelf Science 131 (2013) 310–318

Contents lists available at SciVerse ScienceDirect

Estuarine, Coastal and Shelf Science

journal homepage: www.elsevier.com/locate/ecss

Systematic non-conservative behavior of molybdenum in a macrotidal estuarine system (Aulne-Bay of Brest, France)

M. Waeles*, G. Dulaquais, A. Jolivet, J. Thébault, R.D. Riso

Université de Brest, IUEM, LEMAR UMR 6539, Place N. Copernic, 29280 Plouzané, France

ARTICLE INFO

Article history:
Received 28 March 2013
Accepted 21 June 2013
Available online 9 July 2013

Keywords:
molybdenum
macrotidal estuary
non-conservative behavior
water column
pore waters
Aulne
Bay of Brest

ABSTRACT

In this study, we focused on the behavior of molybdenum in a macrotidal estuarine system (Aulne-Bay of Brest, France). A systematic and pronounced loss of dissolved molybdenum was observed in the inner part of the system which was ~10–30 fold higher than the inputs from the fluvial waters. Further to the examination of Mo concentrations in the water column and in the sediment pore waters over a 6-month period at a coastal station, we found that the systematic deficit in Mo concentrations in the coastal area was related to the loss of metal in the inner part of the system. We also estimated that benthic inputs in the downstream part of the system could be sufficient to counterbalance the upstream losses. After its incorporation in particles within the high turbidity area of the estuary, we postulate that Mo is redistributed downward following the deposition of the particles in areas of sedimentation and the redissolution of Mo in pore waters.

© 2013 Elsevier Ltd. All rights reserved.

1. Introduction

In relation to the high stability of its main chemical form in solution (i.e., molybdate ion: MoO_4^{2-}), molybdenum has a relatively long residence time (~8.10^5 years) and is the most abundant transition metal in the Ocean. Molybdenum is involved in the catalysis of nitrate reduction and nitrogen fixation (Cole et al., 1993). Despite this important biological role, Mo appears conservative in seawater (Emerson and Huested, 1991; Morford and Emerson, 1999) because of its relatively high concentration (~110 nM) that is far in excess to that required by planktonic species. The conservative behavior of Mo was highlighted by pioneer studies of Morris (1975) and Collier (1985) in the Atlantic and Pacific Ocean. More recently, Tuit (2003) also found conservative behavior in open Ocean but also evidenced some deviations close to margins (i.e. in the Eastern Tropical Pacific and off California) that were related to interactions with sediments.

According to the oceanic flux mass balance reported by Morford and Emerson (1999), the main Mo sources are essentially rivers and continental margin sediments whereas Mo loss is found mainly in deep sea sediments and anoxic sediments. The estimation of the riverine flux (Martin and Meybeck, 1979), which represents at least 90% of the inputs, is based however on the assumption of conservative behavior in estuaries thus ignoring the biogeochemical and sedimentological processes potentially affecting the fate of Mo in these systems.

In estuaries, dissolved molybdenum (DMo) concentrations are usually between ~1 nM and ~110 nM as the result of mixing between lower concentrated river end-member and seawater. DMo has been considered as behaving conservatively in estuaries (Shiller and Boyle, 1991 and references therein). However, among the few studies that have examined its distribution in estuarine gradients (Head and Burton, 1970; Van der Sloot et al., 1985; Khan and Van Den Berg, 1989; Shiller and Boyle, 1991; Dalai et al., 2005; Strady et al., 2009; Wang et al., 2009; Rahaman et al., 2010), various more or less important deviations from mixing line were observed.

If some deviations appeared to be related to processes occurring at low salinities (i.e., $S < 15$), as in the Tamar estuary (Khan and Van Den Berg, 1989) and in the Hooghly estuary (Rahaman et al., 2010) where concave DMo-salinity distributions suggested DMo removal, most of the studies evidenced deviations due to processes occurring at high salinities/coastal waters. Different mechanisms have been proposed for explaining DMo deficit in these waters. In their study of the Saanich Inlet, Berrang and Grill (1974) reported DMo concentrations in the range 73–107 nM and suggested Mo scavenging by freshly

* Corresponding author.
E-mail address: waeles@univ-brest.fr (M. Waeles).

0272-7714/$ – see front matter © 2013 Elsevier Ltd. All rights reserved.
http://dx.doi.org/10.1016/j.ecss.2013.06.018

formed MnO_x phases. Such a mechanism involving MnO_x phases has been conceptualized by Adelson et al. (2001). In their model, Mn being reductively dissolved within the sediment or within the water column (depending on anoxia conditions), is refluxed above and reacts with molybdate ion (MoO_4^{2-}) thus concentrating Mo in particulate MnO_x phases. In the Seto Inland Sea, Yamazaki and Gohda (1990) found DMo concentrations in the range 70–120 nM and DMo deficits, which were only observed in summer, were attributed to a scavenging of Mo as an organically associated species. In the same way, Head and Burton (1970) observed DMo deficits in the marine part of the estuary of Southampton water during spring which was linked to complexation by organic particles and/or utilization by phytoplankton. Although less common, it is worth noting that positive anomalies were sometimes observed. For example, Dalai et al. (2005) reported excess of DMo across the Chao river estuary which were driven by mixing with deep coastal waters strongly enriched by Mo additions from suboxic diagenesis in sediments. Positive anomalies were also reported by Strady et al. (2009) in the high-salinity section of the Gironde estuary. Because they observed higher DMo concentrations near the bottom, Strady et al. attributed this excess to inputs from interstitial water and/or to resuspension of Mo rich particles. The study by Dellwig et al. (2007) of the Wadden Sea is probably the most meaningful for understanding DMo deviations in coastal waters. These authors showed that the strong decline in DMo concentrations they observed in summer (with DMo values in the range 40–80 nM) was linked the decomposition of phytoplankton by bacteria which releases organic compounds that promote aggregation of suspended mineral particles. They thus proposed that molybdate ion could be scavenged by freshly formed organic particles and/or reduced in oxygen-depleted aggregates. Dellwig et al. (2007) also showed that decomposition of these aggregates on tidal flats leads to release of Mo from sediments thus replenishing the Mo pool in the water column. It is worth noting that the reported Mo-salinity distributions are generally hard to analyze in terms of deviation from linearity rendering interpretation of Mo behavior difficult and not permitting reliable flux quantifications.

Here we report the distribution of Mo in the salinity gradient of a temperate macrotidal estuary (Aulne estuary, Bay of Brest) with the aim to describe the Mo behavior under various hydrological conditions. During this 6-month study (Jan–Jun 2011), a high frequency sampling was also realized at a fixed site (Lanvéoc) in order to quantify the exchanges between the water-column and sediment pore waters.

2. Material and methods

2.1. Study area

The Aulne River, which is by far the main River discharging into the Bay of Brest (48°20′N; 04°20′W), is 130 km long and has a drainage basin of 1850 km^2. It collects the waters from a poorly industrialized catchment with agricultural areas and meadows representing the majority of the soil occupancy. The water discharge at Châteaulin usually fluctuates in the range 5–80 $m^3\ s^{-1}$ (average 21 $m^3\ s^{-1}$). Evolution of the water discharge is constrained by a temperate oceanic climate. Rain falls the year round (annual rainfall in the range 700–1600 mm), with a distinct maximum during winter, mainly from the regular procession of weather fronts that move eastwards across the Atlantic. As a result, ~60% of the annual flow generally occurs in the December–March period. The estuary is situated downstream of Châteaulin (Fig. 1), covering a distance of ca. 30 km, but with a plume extension covering a great part of the Bay of Brest during winter. It is subjected to a macrotidal regime as the tidal range fluctuates between 1.2 m and 7.3 m. The residence time of water within the estuary, which is highly dependent on the tide and the river flow, varies between 3 days and 30 days (Bassoullet, 1979). The Bay of Brest is a 180 km^2 semi-enclosed marine system connected to shelf waters (Iroise Sea) by a narrow (2 km wide) and deep (40 m) strait. The bay is relatively shallow with an average depth of 8 m.

2.2. Sampling

Fig. 2 summarizes the evolution of water discharge and indicates the date of each sampling campaign over the studied period. Five cruises were conducted for sampling the estuary during the January–June 2011 period (25 Jan, 10 Feb, 24 Mar, 12 Apr and 24 May) from a speed aluminium boat (Hesione, INSU-CNRS-UBO). Stations were selected with the aim of covering the freshwater–seawater mixing zone. Sampling, which was realized under intermediate tidal range (i.e. 2.5–5 m), was performed by starting in the upstream section around high tide time. Then samples were taken downstream (within 1 h) in order of increasing salinities. Water was sampled by hand at ca. 0.3 m below the surface with the arm fully covered with a plastic glove (92 cm, Polysem®). Bottles

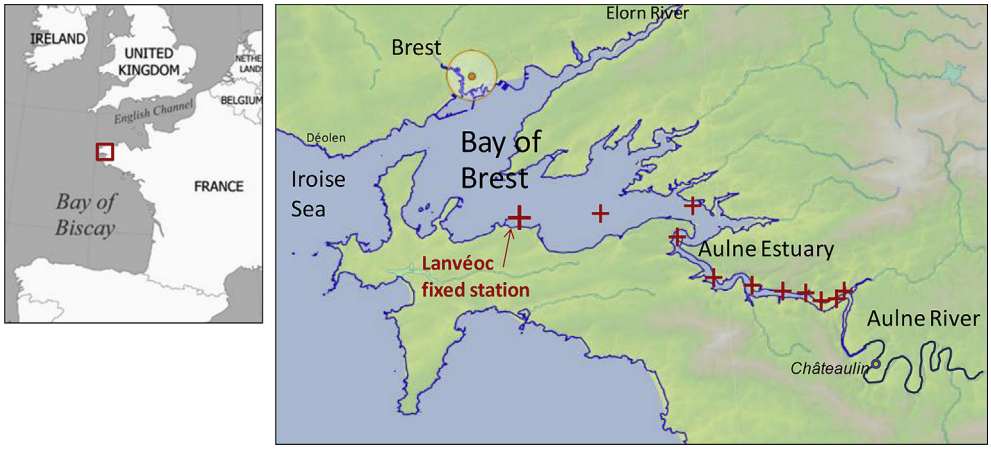

Fig. 1. Study area (Aulne estuary, Bay of Brest). Crosses indicate approximate position of stations for the first sampling campaign (25 Jan 2011). For other campaigns, position of stations were slightly different but were also selected with the aim of covering the whole salinity gradient.

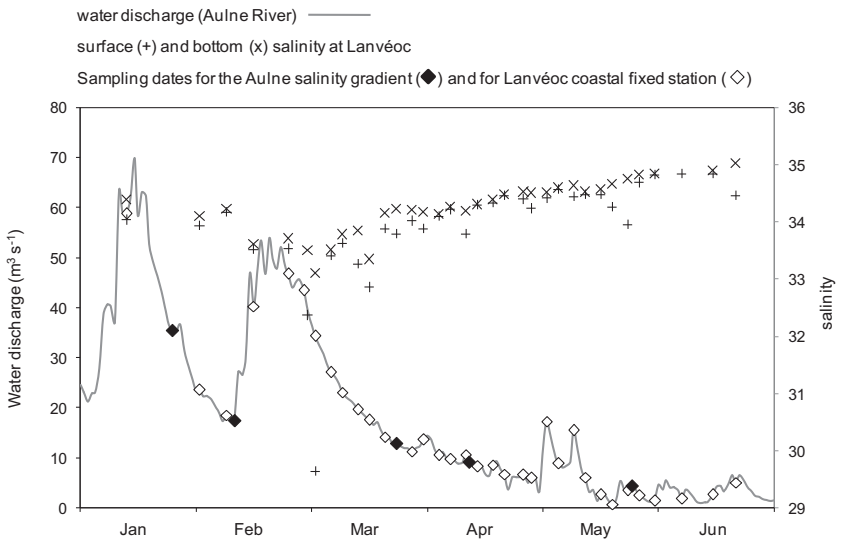

Fig. 2. Variations of the Aulne River water discharge (Châteaulin station, Agence de l'eau Loire Bretagne) and salinity at Lanvéoc coastal station (surface and bottom) over the January–June 2011 period. Black diamonds indicate dates of sampling campaign realized along the salinity gradient (Aulne estuary). White diamonds indicate dates of sampling at the fixed station of Lanvéoc.

used were 1 L HDPE (Nalgene®). Salinity (S) and temperature were recorded with a WTW ProfiLine LF 197 probe (±0.1 and 0.1 °C precision, respectively). Over the same period, 34 cruises were also realized on a weekly-basis at the fixed station of Lanvéoc (Fig. 1). Water samples were collected with 12 L Niskin bottles at three depths (surface, mid-depth, and bottom) from the Albert Lucas boat (INSU-CNRS-UBO). Salinity and temperature profiles were obtained from a SeaBird SB19 probe with a precision of ±0.005 and 0.02 °C, respectively. Sediment cores were also sampled at this site from end of February onwards. This sampling was done by SCUBA diving using Plexiglas cylindrical tubes (length 30 cm and diameter 5.5 cm). Overlying water thickness was ~5 cm. This value of ~5 cm was kept as constant as possible.

2.3. Sample treatments and reagents

Water column samples were filtered in the laboratory within 2 h of collection. To separate the dissolved fraction from the suspended particles, samples were filtered through 0.45 μm mixed cellulose esters filters (diameter 47 mm, HATF type, Millipore®). The filtrate was then acidified to pH 2 (HCl, suprapur®, Merck), UV-irradiated for 45 min (100-W high-pressure mercury vapor lamp surrounded by four 30 mL quartz tubes capped with PTFE stoppers) and stored at 4 °C in HDPE flasks (Nalgene) until further analysis of dissolved Mo (DMo).

Filters were placed in 30 mL PFA closed vessel (Savillex) and digested with 2 mL HNO_3 65% (suprapur, Merck) at 100 °C for 4 h. Nitric acid solution were then diluted to a concentration of 2.5% for further analysis of particulate Mo (PMo) and particulate Pb (PPb). It is worth reminding here that such digestion (Townsend et al., 2001; Sastre et al., 2002) is not sufficient to dissolve the aluminosilicate material. Consequently, PMo and PPb do not represent total particulate concentrations.

Sediment cores were processed in the laboratory within 3 h after collection. Pore waters were extracted from the top 5 cm of the core with Rhizon (0.1 μm pore size) samplers at 1 cm interval. At the same time, overlying water was gently sampled with a PE syringe and immediately filtered as water column samples. Pore waters and overlying waters were then stored in 15 mL PP centrifuge tubes (Elkay) until analysis of DMo.

Prior to use, all the items employed for sampling, filtration and sample storage were washed with ultrapure water (>18 MΩ) from a Milli-Q Element system (Millipore, Billerica, MA, USA), then and for at least 72 h with diluted hydrochloric acid (pH 2, HCl suprapur, Merck) and finally rinsed several times with ultrapure water. All filtrations, sediment cores processing, sample preparation and electrochemical analyses were carried out in a class-100 laminar flow hood.

2.4. Analyses and standard solutions

Voltammetric measurements of DMo were performed with a potentiostat/galvanostat μ-Autolab III unit controlled by GPES 4.9 software and operating on a three electrode basis in a quartz cell. The working electrode was a static mercury drop electrode (SMDE), Metrohm model 663 VA, with a mercury drop size of 0.52 mm^2. An Ag/AgCl (3 M KCl, Suprapur) electrode and a platinum electrode were used as the reference and the auxiliary electrodes, respectively. Analysis was conducted by differential-pulse adsorptive voltammetry according to the method described in Quentel et al. (1992). This method is based on adsorption of a complex formed by Mo with fulvic acid (FA) and 1,10 phenanthroline (phen). In order to control the concentration of FA in the sample, which is a critical parameter for staying in the linear range of the method (Quentel and Elleouet, 2001), the samples need to be UV-irradiated. FA and phen are added to the acidified/UV-irradiated sample at concentrations of 150 μg L^{-1} and 1.0 10^{-4} M, respectively. The sample (~20 mL) is then deaerated with nitrogen for 10 min. A potential of −0.25 V (vs Ag/AgCl/KCl, 3M) is applied under stirring (Teflon rod) with allowing the simultaneous formation/adsorption of the Mo(VI)-FA-phen complex and its subsequent reduction to Mo(V)-FA-phen at the mercury drop. Typical adsorption time is 60 s–180 s. After a 10 s equilibration time, stripping is performed in the differential-pulse mode using the following operational parameters. Initial potential: −0.15 V; Final potential: −0.75 V; Pulse time: 50 ms; Pulse rate: 2 s^{-1}; Step potential: 2 mV; Pulse amplitude: 50 mV. Under stripping, the previously adsorbed Mo(V)-FA-phen complex is reduced to Mo(IV)-FA-phen and desorbs from the mercury drop. Details of the involved mechanism are given in Quentel (1999). DMo analyses were conducted after dilution in

ultrapure water. Typical dilution factors were 20–25 for pore waters and 3–5 for water column and sediment overlying waters. DMo concentrations are determined after 3 standard additions of the same standard solution. The reliability of the method was checked by five analysis of a NASS-5 (National Research Council Canada) certified reference seawater. Obtained concentration was 94 ± 4 nM (Certified value: 100 ± 10 nM) giving a precision under 5%. A precision under 5% was also obtained at a level of ~25 nM (i.e. 24.8 ± 1.2 nM, $n = 5$). Mo(VI) standard solutions (10 μM and 2 μM) were prepared in 0.01 M HCl from a 1000 mg L^{-1} standard solution (Fluka). FA standard was prepared in 10^{-2} mol L^{-1} NaOH (Suprapur, Merck) by weighing the appropriate mass of the R 1S101F-IHSS standard powder (International Humic Substance Society). From this stock solution (470 mg L^{-1}), a working solution (19 mg L^{-1}) was done in HCl 0.01 M. 1,10 phenanthroline standard was prepared by dissolving the appropriate amount of 1,10 phenanthrolinium chloride in 0.01 M HCl.

PMo and PPb were determined using a Quad Xseries2 (ThermoFisher Scientific) ICP-MS (Pôle Spectrométrie Océan, IUEM-UBO) with a precision under 0.5% and a quantification limit of 40 and 70 pM, respectively. Isotopes used for quantification were ^{97}Mo and ^{208}Pb because of negligible potential interferences (i.e., $^{57}Fe^{40}Ar$, $^{168}Er^{40}Ar$ and $^{168}Yb^{40}Ar$). ^{97}Mo measurements were very consistent with ^{95}Mo measurements. Standard solutions for ICP-MS were prepared from 1000 mg L^{-1} elemental standard solutions (Fluka) in HNO_3 2.5%. All standards were prepared in ultrapure water. Reliability on PMo and PPb measurements were checked on a certified reference sediment (PACS-2, National Research Council Canada). This sediment (10 replicates) was digested and analyzed according to the above described procedures. For Mo and Pb, concentrations of 4.64 ± 0.55 and 191 ± 22 μg g^{-1}, respectively, have been obtained (certified values: 5.43 ± 0.28 and 183 ± 8 μg g-1, respectively).

2.5. Interpretation of estuarine mixing diagrams

The non-conservative mixing was tested by fitting a second-order polynomial model ($DMo = aS^2 + bS + c$) to each set of data (Rochelle-Newall and Fisher, 2002). In order to determine whether this model gives a significantly better fit to the data than the linear model ($DMo = a'S + b'$), corresponding to a conservative mixing, an F-test was then conducted. F_{exp} was given by:

$$F_{exp} = \frac{\frac{SS_1 - SS_2}{p_2 - p_1}}{\frac{SS_2}{n - p_2}}$$

where SS_2 and SS_1 are the residual sum of squares and p_2 and p_1 are the number of parameters of second-order model and linear model, respectively; n being the number of data points. For rational reason, it is worth mentioning that intercept was fixed to zero when the first fitting gave negative intercept. The null hypothesis, i.e., second-order model not providing a better fit than linear model, is rejected if F_{exp} is greater than the critical value of the F distribution for a 0.05 false-rejection probability. Under this null hypothesis, the mixing was considered as being not significantly non-conservative.

2.6. Quantification of DMo deficits and DMo fluxes

DMo deficit (absolute or relative value) was quantified, at a given salinity, by difference between (i) the expected value for a conservative mixing between the fluvial end-member (DMo = 1 nM) and the oceanic end-member (DMo = 107 nM, Morris, 1975) and (ii) the measured concentration.

Three types of fluxes were quantified: DMo inputs from the river, DMo loss in the inner estuary and DMo inputs from sediment pore waters at the coastal station of Lanvéoc.

- Inputs from the river were estimated from DMo average concentrations obtained at salinity 0 (i.e., 1.5 ± 1.1 nM, $n = 4$). By multiplying this concentration by the average water discharge during the studied period (i.e. 16 m^3 s^{-1}), this gives a DMo flux of ~2 ± 2 mol day^{-1}. Uncertainties are obviously important for this estimation. Estimation of this flux by another type of calculation, using daily fluvial concentrations and daily discharge for example, gives 3 ± 3 mol day^{-1} but the aim here was only to point out that this flux is low as compared to other fluxes.
- For quantifying DMo loss during estuarine transport, tangents to the second-order models at $S = 30$ were calculated and the intercepts (a_i^*) were considered to represent the effective zero-salinity end member (Officer, 1979). Then, DMo losses were obtained by multiplying each effective zero-salinity end member by the appropriate water discharge.
- The magnitude of diffusive release was estimated using a modification of Fick's first law of diffusion appropriate for sediments (Berner, 1980):

$$F_{sed} = \Phi^* D^* \frac{\Delta C}{\Delta z}$$

Where φ is the porosity of the sediment determined as the weight loss from fresh sediment dried at 100 °C for 24 h ($\varphi = 58 \pm 7\%$). D is the diffusion coefficient of the molybdate ion (D = 5–10 10^{-6} cm^2 s^{-1}; Yuan-Hui and Gregory, 1974; Crusius et al., 1996). $\Delta C/\Delta z$ is the assumed linear concentration gradient for each core profile. $\Delta C/\Delta z$ has been estimated from the slope of the linear regression between concentrations and sediment depth. 95% confidence interval of each slope was also calculated and taken into account for flux errors.

3. Results and discussion

3.1. Inner estuary

Dissolved molybdenum (DMo) concentrations in the estuary ($S < 30$) are displayed as a function of salinity for each sampling campaign (Fig. 3). Concentrations were in the range 1–90 nM with a gradual increase from fluvial to marine waters in accordance with other reports conducted in estuarine systems (e.g. Head and Burton, 1970; Dalai et al., 2005). Particulate molybdenum (PMo) concentrations (Fig. 4A) were in the range 0.06–3.3 nM with high concentrations (i.e. PMo>0.3 nM) being found in the salinity range 0–10. Although SPM concentrations were not measured here, it is worth noting that an excellent relationship was obtained between SPM and PPb in the Penzé estuary (a closed and very similar system including in term of Pb levels). This relation (given in Tanguy et al., 2011 Marine Freshwater Research 62,1–13) is SPM(mg L^{-1}) = 3.2 PPb(nM)-5.8, $R^2 = 0.994$, $n = 42$). Thus PPb values can be viewed as a good estimator for SPM concentrations. Fig. 4B shows that PMo concentrations are well correlated to that of PPb (PMo(nM) = 0.0022 PPb(nM)+0.096, $R^2 = 0.94$, $n = 63$) and thus high PMo values in the salinity range 0–10 are linked to the maximum turbidity zone (MTZ). According to Bassoullet (1979), suspended particulate matter concentrations in the MTZ varied usually within the range 30–500 mg L^{-1}. In this part of the estuary, PMo represented a relatively high proportion of total Mo (1–78%). At higher salinities ($S > 10$), PMo was always less than 1% of total Mo (mean ± sd: 0.3 ± 0.3%).

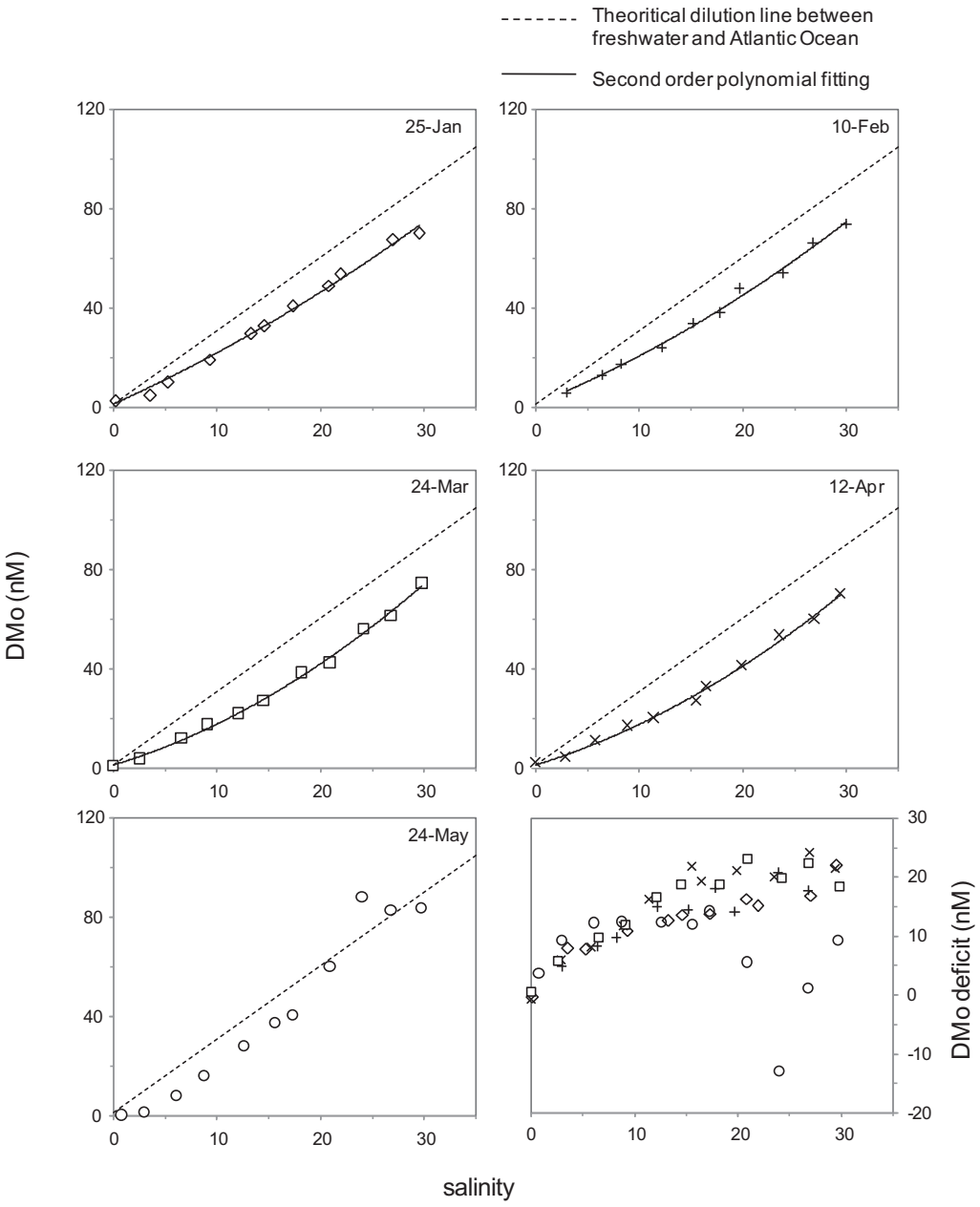

Fig. 3. Dissolved Mo (DMo) concentrations as a function of salinity for each sampling campaign conducted in the Aulne estuary. Dotted line represents the theoretical mixing line between fluvial waters (DMo = 1 nM) and the Atlantic Ocean end-member (DMo = 107 nM, Morris, 1975). DMo deficit for each sampling campaign are presented in the last panel.

The particularity of the Mo-salinity distribution was the concave shape obtained for each data set suggesting a non-conservative behavior. In order to validate this hypothesis, F-tests have been applied (Table 1). F_{exp} value was generally greater than F_{th} value (occurrence 4/5) thus clearly demonstrating than DMo behaved non-conservatively and than a loss of DMo occurred systematically during estuarine mixing. The exception of the 24-May data set in term of F-test result cannot rule out this assumption because a concave shape was also obtained in the low salinity section of the estuary. The DMo deficit was quantified on each point by comparison with the theoretical dilution line between fluvial waters (DMo = 1 nM, this value being is approximately the average concentration obtained in this study) and the Atlantic Ocean end-member (DMo = 107 nM, Morris, 1975). Fig. 3 (last panel) shows that this deficit is in the range 0–25 nM and generally increased as a function of salinity. Note that the increase was particularly high in the salinity range 0–10 (from 0 to 10 nM). Because the residence time of the waters in this salinity section (~ 0.3 day, Bassoullet, 1979) is low as compared to the remaining system (~3 and 100 day, for the salinity sections 10–20 and 20–30, respectively), the removal rate of DMo should be much higher in this area which corresponds to the MTZ. It should be noted that DMo deficit expressed as relative values was clearly more important under high PPb concentrations (Fig. 4D).

In the Aulne estuary, the DMo removal, which was observed on each profile, is clearly driven in the inner estuary (i.e., $S < 10$). Such a removal occurring at low salinity was actually observed in very few systems. This includes the Tamar estuary (Khan and Van Den Berg, 1989) and the Hooghly estuary (Rahaman et al., 2010) where DMo deficits (~30% for each system) are interestingly closed to those observed in the Aulne. It should be noted that these two systems are also macrotidal with suspended particulate matter

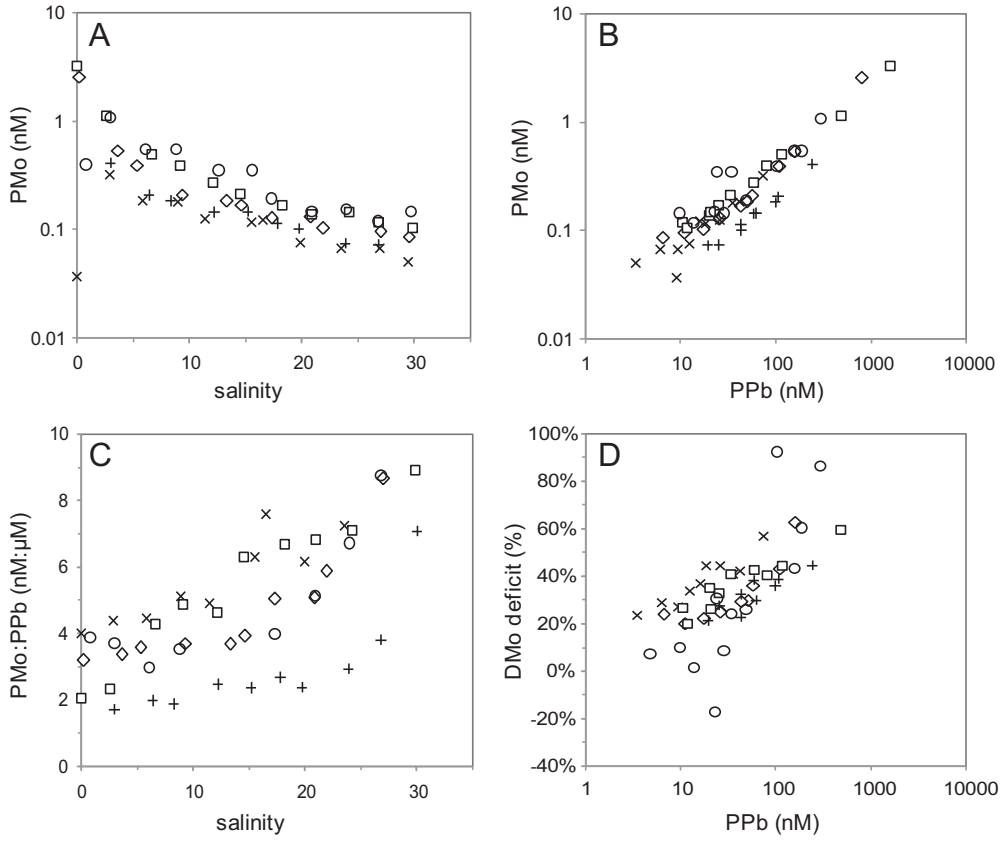

Fig. 4. (A) particulate Mo (PMo) concentrations as a function of salinity, (B) PMo concentrations as a function of particulate Pb (PPb) concentrations, (C) PMo:PPb ratio as a function of salinity, (D) DMo relative deficit as a function of PPb concentrations. On each panel, all sampling campaigns conducted in the Aulne estuary are displayed, see Fig. 2 for legend.

concentrations commonly exceeding 100 mg L^{-1} at low salinities (Uncles and Stephens, 1993; Mukhopadhyay, 2007). Although sampling on the Tamar and the Hooghly estuaries were restricted to one survey, the removal of DMo at low salinities may be a common feature of macrotidal systems. In their intensive study of the Gironde estuary, another macrotidal system with important SPM charges, Strady et al. (2009) also found several times a DMo subtraction. Although their observations cannot dismiss a DMo removal driven within the MTZ (see our explanations about the residence time of the waters in such area of the system), these authors actually located the losses at mid salinity, downstream the MTZ, and thus attributed them to primary production. In contrast to our system, important additions, well exceeding the theoretical dilution line between fluvial and Atlantic waters, were also occasionally observed at mid and high salinities in the Gironde. Although very substantial, these additions did not produced positive anomalies in the MTZ, suggesting that removal is dominating in the MTZ.

Some of the mechanisms proposed for Mo scavenging include: the authigenic precipitation of Mo in polyframboids (iron sulfide microniches, Strady et al., 2009), and association of Mo with humic-bond thiol groups that can "switch" Mo behavior from conservative to particle-reactive element (Helz et al., 1996). According to their measurement of the Mo labile fraction, Khan and Van Den Berg (1989) suggested that a great part of Mo could be associated with colloids or organically complexed. In a recent study, also conducted on a macrotidal estuary (Tanguy et al., 2011), we demonstrated that flocculation of organomineral colloids was the major mechanism for explaining the strong Pb removal at low salinities. The strong correlation found between PMo and PPb for each survey (although being principally driven by the suspended particulate charge, Fig. 4B) and also the link observed between DMo removal and PPb concentrations (Fig. 4D) suggest that such a mechanism or a mechanism associated with should be considered for interpreting Mo scavenging. Indeed, the PMo:PPb ratio increase as a function of salinity (Fig. 4C) put forward a mechanism in which Mo could be also adsorbed on these newly formed particles. Note that higher PMo:PPb increases which were observed in March and April corresponded to the stronger DMo deficits.

Table 1
Results of DMo-S fitting with second-order model (DMo = aS^2+bS + C) and linear model (DMo = a'S + b') for each sampling campaign. F_{exp} and F_{th} are values of the F-test which was conducted for demonstrating the non −conservativity of DMo; a_i^* is the effective zero-salinity end-member concentration (nM).

Sampling date	Second-order DMo-S fitting	R^2	Linear DMo-S fitting	R^2	n	F_{exp}	F_{th}	a_i^*
25 Jan	DMo = 0.0140S^2+2.06S	0.994	DMo = 2.38S	0.990	11	6.1	5.1	−13
10 Feb	DMo = 0.0243S^2+1.76S + 0.50	0.995	DMo = 2.34S	0.98	9	11	5.6	−25
24 Mar	DMo = 0.0375S^2+1.31S + 1.06	0.997	DMo = 2.24S	0.97	11	69	5.1	−38
12 Apr	DMo = 0.0367S^2+1.24S + 1.86	0.996	DMo = 2.18S	0.97	11	44	5.1	−40
24 May	DMo = 0.0497S^2+1.72S	0.95	DMo = 2.88S	0.92	11	4.5	5.1	−37

3.2. Outer estuary and coastal area

At the coastal fixed station of Lanvéoc, DMo concentrations in the water column (surface, mi-depth and bottom, Fig. 5, upper panel) varied between 56 and 107 nM (mean ± sd: 80 ± 12 nM, $n = 101$). Given the salinity values recorded at this station (range 32–35, Fig. 2), DMo concentrations were generally significantly below those expected for a conservative mixing (DMo deficit: 25 ± 11%, $n = 101$). Vertical differences were low but a closer examination indicates that subsurface concentrations were often lower than bottom concentrations (occurrence 27/34). Temporal variations show a distinct period, i.e. March–April, when lower DMo concentrations and conversely higher DMo deficits were observed. Before this period (i.e. January–February), DMo concentrations were 80 ± 5 nM (DMo deficit: 26 ± 4%, $n = 14$). Then, DMo concentrations dropped to 71 ± 5 nM in March–April (DMo deficit: 35 ± 8%, $n = 54$) and increased to be 91 ± 9 nM during the May–June period (DMo deficit: 17 ± 8%, $n = 33$). Sediment overlying concentrations, which are displayed in both panels, were 92 ± 15 nM (DMo deficit: 14 ± 14%, $n = 28$) and thus significantly higher than those of the water column. Concentrations in pore waters within the first 5 cm of the sediment (Fig. 5, lower panel) were even more elevated (mean ± sd: 170 ± 120 nM, $n = 102$, with 75% of the DMo measurements exceeding 100 nM) and generally increased with depth. However, one should note the particularity of end of May to early June period when much lower concentrations were observed (i.e. below 100 nM through the 0–5 cm depth section).

At our coastal station of Lanvéoc, DMo concentrations recorded between January and June 2011 were always below those expected for a conservative mixing between fluvial and oceanic end-members. To our knowledge, this is the first time that a deficit in DMo concentrations is observed over such a long period of time. An important outcome from this result is that a substantial part of the DMo deficit found in the outer estuary/coastal area should be first linked to the DMo removal driven within the inner estuary and which is related to the high suspended matter load of this macrotidal estuary. Other processes in relation with phytoplankton dynamic, although possibly superimposed in some occasions, are hardly conceivable over the whole studied period.

In the outer estuary/coastal area, one would expect that salinity also exerts a certain control on DMo levels. This is evidenced by the relatively good correlation obtained for the whole data set obtained at this station (DMo = 11.9S-330, $R^2 = 0.27$, $n = 100$, $p < 10^{-7}$). This control by salinity is however limited to temporal variations. Indeed, DMo differences between depth levels were not correlated with salinity differences between depth levels. As an example, the obtained linear regression between bottom and subsurface differences (hereby referred as ΔDMo and ΔS) was poor (ΔDMo = −1.8ΔS+5, $R^2 = 0.011$, $n = 34$, $p = 0.55$). Stratification of the waters (see differences between subsurface and bottom salinity in Fig. 2) is probably too low for explaining DMo differences between depth levels. Inputs from sediment could be more important for generating higher DMo levels in bottom waters.

3.3. Fluxes and conceptual cycle of Mo in macrotidal estuaries

Intercepts of the second order model (also displayed in Table 1), which were used for quantifying DMo loss, were always negative and varied between −13 nM and −40 nM. According to Officer (1979), this can be interpreted as the conjunction of an input from marine waters that enters the system and a loss, within the system, exceeding this input. It is worth also noting that March and April were characterized by the lowest intercepts thus explaining the higher DMo deficits recorded at the coastal station over the March–April period. Benthic inputs at the coastal station (Fig. 6), which varied between −100 and 400 nmol m^{-2} day^{-1}, were generally positives thus indicating a DMo release from the sediment to the overlying waters. For the studied period, and by using uncertainties on diffusion coefficient of molybdate ion and porosity (see section 2.6), this gives a mean flux between 60 and 160 nmol m^{-2} day^{-1}.

Important points can be deduced from our flux calculations. At first, DMo loss is much more important (i.e. 10–30 fold higher) than inputs from the fluvial waters (~2 mol day^{-1}). This indicates that macrotidal systems can eventually represent a substantial sink of Mo at a global scale. This assumption is supported by the study of Rahaman et al. (2010) in which they demonstrated important Mo removal in the Hooghly and the Mandovi estuaries, although attributing this removal to processes associated with the mangrove swamp and not the high suspended particle charge of the systems. Secondly, the high DMo removal observed in our estuary is probably counterbalanced by benthic inputs occurring downstream. After its incorporation in particles within the high turbidity area of the estuary, we postulate that Mo is redistributed downward following (i) the deposition of these particles in areas of

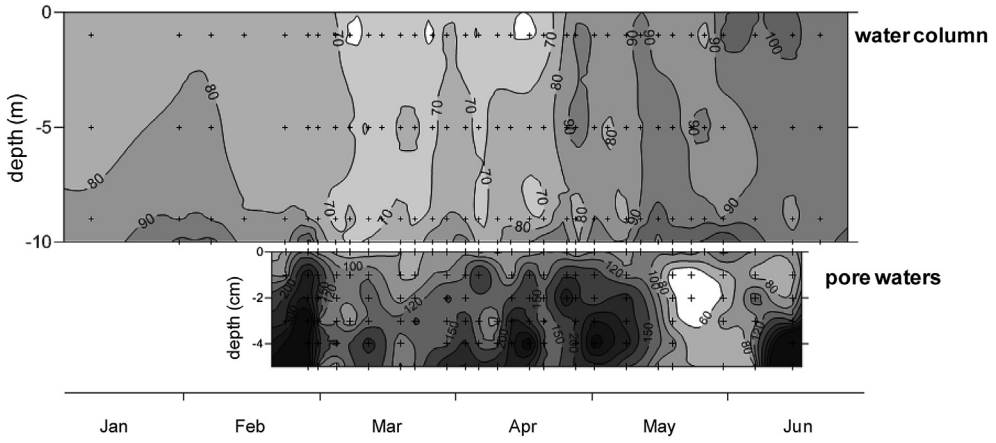

Fig. 5. Vertical distribution of dissolved Mo (DMo) as a function of time at the fixed coastal station of Lanvéoc. Upper panel: water column concentrations (concentrations at 10 m correspond to sediment overlying waters); lower panel: sediment pore waters concentrations (concentrations at 0 cm correspond to sediment overlying waters). The figure was made with Surfer 9 (Golden Software); a linear kriging was applied with anisotropy of 0.5 and 1 for upper and lower panel, respectively.

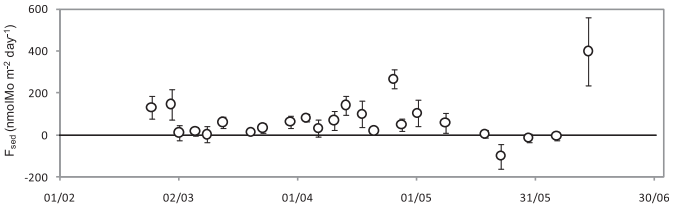

Fig. 6. Dissolved Mo fluxes by diffusive release from the benthic compartment to the water column at the coastal station of Lanvéoc.

sedimentation and (ii) the redissolution of Mo in pore waters. It is worth noting that benthic inputs could also exist in the inner estuary but, based on the DMo-salinity distributions only, it is not possible to detect them and indeed such inputs are probably limited in comparison to DMo loss.

According to our measurements at the coastal station of Lanvéoc, an area of ~300–900 km^2 would be necessary for producing benthic Mo inputs matching the Mo removal within the inner estuary. Although this represents an area about one order of magnitude higher than the area under influence of particle deposition from the Aulne estuary (Bassoullet, 1979), it is worth reminding here that (i) our estimation is based on a unique station and that (ii) this station is situated downward the area directly influenced by high particle depositions thus being probably characterized by lower Mo inputs. An assumption that higher Mo inputs could occur upstream is supported by the May DMo-salinity distribution in which high DMo inputs are clearly observed at salinity of ~25. We thus anticipate that a substantial part of Mo being trapped in particles is not definitively sequestered. The high ratio between DMo removal and fluvial inputs (i.e. 10–30) actually suggest that Mo is recycled several times by the above described mechanism before being exported toward the ocean. A mass balance of Mo in the Aulne estuary is described in Fig. 7. Note that this mass balance, based only on our measurements, remains incomplete. As indicated above, additional sampling along the salinity gradient will be necessary to establish the veracity of the benthic inputs in such macrotidal system and also to test if macrotidal systems represent actually a sink for Mo of both riverine and marine origin as suggested by the result of this study.

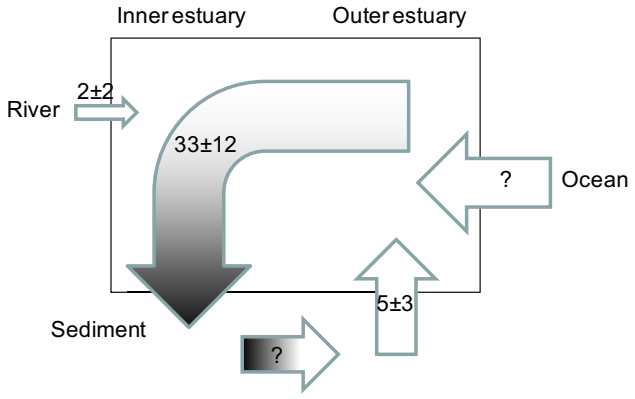

Fig. 7. Mass-balance of Mo in the Aulne estuary based on our flux calculations (fluxes in mol day^{-1}). White and black colors correspond to dissolved Mo (DMo) and particulate Mo (PMo), respectively. Loss of Mo in the inner system (i.e. 33 ± 12 mol day^{-1}) is the mean (±sd) of each sampling campaign loss. Input from sediment was assessed using 50 km^2 which is approximately the surface of the area influenced by particle deposition (Bassoullet, 1979). (For interpretation of the references to color in this figure legend, the reader is referred to the web version of this article.)

4. Conclusion

In this study, a systematical non-conservative behavior for dissolved Mo is demonstrated for the first time. An important loss was observed within the inner part of the estuary which was ~10–30 fold higher than inputs from fluvial waters thus revealing a much more dynamic behavior for Mo than previously thought, at least for macrotidal systems. Our data indicates that such a removal can account for the majority of the dissolved Mo deficit observed in the outer estuary/coastal area. Further investigations are needed to elucidate the exact nature of the involved process in DMo loss within the high turbidity area and DMo release in sediments. Thorough examination of bigger estuarine systems are also required to assess whether Mo scavenging and release in macrotidal systems may affect the oceanic budget of this element.

Acknowledgments

We would like to thank Isabelle Bihannic and Erwan Amice for their quality assistance in sampling. This project was supported by the French program ANR-Blanc (Agence Nationale de la Recherche-CHIVAS project).

References

Adelson, J., Helz, G., Miller, C., 2001. Reconstructing the rise of recent coastal anoxia; molybdenum in Chesapeake Bay sediments. Geochimica et Cosmochimica Acta 65, 237–252.
Bassoullet, P., 1979. Etude de la dynamique des sédiments en suspension dans l'estuaire de l'Aulne (rade de Brest). Université de Bretagne occidentale. (PhD thesis).
Berner, R.A., 1980. Early Diagenesis: a Theoretical Approach. Princeton University Press.
Berrang, P., Grill, E., 1974. The effect of manganese oxide scavenging on molybdenum in Saanich Inlet, British Columbia. Marine Chemistry 2, 125–148.
Cole, J.J., Lane, J.M., Marino, R., Howarth, R.W., 1993. Molybdenum assimilation by cyanobacteria and phytoplankton in freshwater and salt water. Limnology and Oceanography 38, 25–35.
Collier, R.W., 1985. Molybdenum in the northeast Pacific Ocean. Limnology and Oceanography 30, 1351–1354.
Crusius, J., Calvert, S., Pedersen, T., Sage, D., 1996. Rhenium and molybdenum enrichments in sediments as indicators of oxic, suboxic and sulfidic conditions of deposition. Earth and Planetary Science Letters 145, 65–78.
Dalai, T.K., Nishimura, K., Nozaki, Y., 2005. Geochemistry of molybdenum in the Chao Phraya River estuary, Thailand: Role of suboxic diagenesis and porewater transport. Chemical Geology 218, 189–202.
Dellwig, O., Beck, M., Lemke, A., Lunau, M., Kolditz, K., Schnetger, B., Brumsack, H.J., 2007. Non-conservative behaviour of molybdenum in coastal waters: coupling geochemical, biological, and sedimentological processes. Geochimica et Cosmochimica Acta 71, 2745–2761.
Emerson, S.R., Huested, S.S., 1991. Ocean anoxia and the concentrations of molybdenum and vanadium in seawater. Marine Chemistry 34, 177–196.
Head, P., Burton, J., 1970. Molybdenum in some ocean and estuarine waters. Journal of Marine Biological Association UK 50, 439–448.
Helz, G., Miller, C., Charnock, J., Mosselmans, J., Pattrick, R., Garner, C., Vaughan, D., 1996. Mechanism of molybdenum removal from the sea and its concentration in black shales: EXAFS evidence. Geochimica et Cosmochimica Acta 60, 3631–3642.
Khan, S.H., Van Den Berg, C.M.G., 1989. The determination of molybdenum in estuarine waters using cathodic stripping voltammetry. Marine Chemistry 27, 31–42.
Martin, J.-M., Meybeck, M., 1979. Elemental mass-balance of material carried by major world rivers. Marine Chemistry 7, 173–206.
Morford, J.L., Emerson, S., 1999. The geochemistry of redox sensitive trace metals in sediments. Geochimica et Cosmochimica Acta 63, 1735–1750.
Morris, A.W., 1975. Dissolved molybdenum and vanadium in the northeast Atlantic Ocean. Deep Sea Research and Oceanographic Abstracts 22, 49–54.
Mukhopadhyay, S., 2007. The Hooghly estuarine system, NE coast of Bay of Bengal, India. In: Proceedings of the Workshop on Indian Estuaries, NIO, Goa, India.
Officer, C.B., 1979. Discussion of the behaviour of nonconservative dissolved constituents in estuaries. Estuarine, Coastal Marine Science 9, 91–94.
Quentel, F., 1999. Voltammetric study of molybdenum in the presence of phenanthroline. Electroanalysis 11, 1355–1360.
Quentel, F., Elleouet, C., 2001. Square-wave voltammetry of molybdenum-fulvic acid complex. Electroanalysis 13, 1030–1035.

Quentel, F., Elleouet, C., Madec, C., 1992. Synergic effect of fulvic acids on the differential pulse adsorptive voltammetry of the Mo (VI)-phenanthroline complex. Electroanalysis 4, 707–711.

Rahaman, W., Singh, S.K., Raghav, S., 2010. Dissolved Mo and U in rivers and estuaries of India: Implication to geochemistry of redox sensitive elements and their marine budgets. Chemical Geology 278, 160–172.

Rochelle-Newall, E., Fisher, T., 2002. Chromophoric dissolved organic matter and dissolved organic carbon in Chesapeake Bay. Marine Chemistry 77, 23–41.

Shiller, A.M., Boyle, E.A., 1991. Trace elements in the Mississippi River Delta outflow region: behavior at high discharge. Geochimica et Cosmochimica Acta 55, 3241–3251.

Van der Sloot, H., Hoede, D., Wijkstra, J., Duinker, J., Nolting, R., 1985. Anionic species of V, As, Se, Mo, Sb, Te and W in the Scheldt and Rhine estuaries and the Southern Bight (North Sea). Estuarine, Coastal and Shelf Science 21, 633–651.

Strady, E., Blanc, G., Schäfer, J., Coynel, A., Dabrin, A., 2009. Dissolved uranium, vanadium and molybdenum behaviours during contrasting freshwater discharges in the Gironde Estuary (SW France). Estuarine, Coastal and Shelf Science 83, 550–560.

Sastre, J., Sahuquillo, A., Vidal, M., Rauret, G., 2002. Determination of Cd, Cu, Pb and Zn in environmental samples: microwave-assisted total digestion versus aqua regia and nitric acid extraction. Analytica Chimica Acta 462, 59–72.

Tanguy, V., Waeles, M., Gigault, J., Cabon, J.Y., Quentel, F., Riso, R.D., 2011. The removal of colloidal lead during estuarine mixing: seasonal variations and importance of iron oxides and humic substances. Marine and Freshwater Research 62, 329–341.

Townsend, A.T., O'Sullivan, J., Featherstone, A.M., Butler, E.C., Mackey, D.J., 2001. The application of ICP-SMS, GF-AAS and HG-AFS to the analysis of water and sediment samples from a temperate stratified estuary. Journal of Environmental Monitoring 3, 113–120.

Tuit, C.B., 2003. The Marine Biogeochemistry of Molybdenum. Massachusetts Institut of Technology and the Woods Hole Oceanographic Institution. (PhD thesis).

Uncles, R., Stephens, J., 1993. The freshwater-saltwater interface and its relationship to the turbidity maximum in the Tamar estuary, United Kingdom. Estuaries and Coasts 16, 126–141.

Wang, D., Aller, R.C., Sañudo-Wilhelmy, S.A., 2009. A new method for the quantification of different redox-species of molybdenum (V and VI) in seawater. Marine Chemistry 113, 250–256.

Yamazaki, H., Gohda, S., 1990. Distribution of dissolved molybdenum in the Seto Inland Sea, the Japan Sea, the Bering Sea and the Northwest Pacific Ocean. Geochemical Journal 24, 273–281.

Yuan-Hui, L., Gregory, S., 1974. Diffusion of ions in sea water and in deep-sea sediments. Geochimica et Cosmochimica Acta 38, 703–714.